Langmuir
Article
pubs.acs.org/Langmuir

$c(4 \times 2)$ Structures of Alkanethiol Monolayers on Au (111) Compatible with the Constraint of Dense Packing

Oleksandr Voznyy* and Jan J . Dubowski

Department of Electrical and Computer Engineering, Centre of Excellence for Information Engineering (CEGI), Université de Sherbrooke, Sherbrooke, Québec J1K 2R1, Canada

Received December 31, 2008. Revised Manuscript Received April 26, 2009

Using alkanethiol dense packing as a starting point, we have found six prototypical packing structures commensurate with the $(3 \times 2\sqrt{3})$ supercell of the Au (111) surface. Five of the six structures are not compatible with the flat surface conditions but can be fitted to a reconstructed surface. Combined with density functional theory calculations and simulations of grazing incidence X-ray diffraction maps and of scanning tunneling microscopy images, this allowed us to refine and assess the recently proposed models of the $c(4 \times 2)$ self-assembled monolayers involving thiolate−adatom and thiolate−adatom−thiolate species and to propose a new model with four gold adatoms per unit cell.

1. Introduction

Self-assembled monolayers (SAMs) of organic molecules on solid substrates attract a lot of interest for their potential applications in nanofabrication, molecular electronics, bio- and chemical sensing, surface protection, and so forth.[1−3] Resolving the atomistic structure of the SAM is an important step toward understanding the process of its formation and creating monolayers with desired functionality. Alkanethiol SAMs on Au (111) became a prototypical system for studying self-assembly because of their stability and ease of preparation, and have been intensely studied for the last two decades.[4] Nevertheless, the exact structure of these SAMs in the "standing-up" phase remains highly debatable. Experimental determination of the structure is problematic because of the impossibility of direct imaging of the interface between the monolayer and the surface. Early theoretical simulations, assuming an atomically flat surface, proposed several models for the $c(4 \times 2)$ superstructure marginally more stable than the $(\sqrt{3} \times \sqrt{3})R30°$ phase (hereafter, $\sqrt{3}$)[5−10] following the experimental suggestions.[4,11] However, most of them were derived for short chain thiols and were not compared to experimental structural data to convincingly select the preferred model.

Only recently have several experiments explicitly shown that thiol SAMs on Au (111) contain gold adatoms.[12−14] The presence of surface reconstruction introduces additional degrees of freedom for modeling and further complicates determination of the exact structure of the monolayer. Several models involving thiolate−adatom,[15] thiolate−adatom−thiolate,[16−19] and thiolate−vacancy[16−18] species were proposed recently, based on the analysis of different data sets, each having its own drawbacks. Particularly, density functional theory (DFT) is known to have deficiencies in describing van der Waals interactions, and most of the theoretical studies had concentrated on short-chain thiols to avoid this problem.[9,10,17,20,21] However, the $c(4 \times 2)$ structure of interest was never observed experimentally for methyl- and ethylthiolate SAMs, making the short-chain thiols an unreliable model system for resolving the $c(4 \times 2)$ structure. On the other hand, models obtained by fitting to experimental grazing incidence X-ray diffraction (GIXRD) data[16,22] were performed independently of theoretical calculations, sacrificing the thermodynamic stability of the structures for the quality of the fit.

In this work we derive several $c(4 \times 2)$ models using thiol densest packing as a primary constraint, which concurrently has the capability to suggest a surface reconstruction rather than adapt to a predefined one. Comparison to a wide set of experimental data allowed us to exclude some of the previously proposed models and reduce the discussion to two structures.

2. Methodology

We adapt the approach previously proposed by us for thiol SAMs on GaAs (001).[23] Infrared reflection spectroscopy (IRS) data[24,25] and tilt angles obtained from near-edge X-ray

*Corresponding author. E-mail: o.voznyy@usherbrooke.ca.

(1) Love, J. C.; Estroff, L. A.; Kriebel, J. K.; Nuzzo, R. G.; Whitesides, G. M. *Chem. Rev*. **2005**, *105*, 1103.
(2) Schreiber, F. *J. Phys.: Condens. Matter* **2004**, *16*, R881.
(3) Seker, F.; Meeker, K.; Kuech, T. F.; Ellis, A. B. *Chem. Rev*. **2000**, *100*, 2505.
(4) Schreiber, F. *Prog. Surf. Sci*. **2000**, *65*, 151.
(5) Fischer, D.; Curioni, A.; Andreoni, W. *Langmuir* **2003**, *19*, 3567.
(6) Gerdy, J. J.; Goddard, W. A. *J. Am. Chem. Soc*. **1996**, *118*, 3233.
(7) Li, T. W.; Chao, I.; Tao, Y. T. *J. Phys. Chem. B* **1998**, *102*, 2935.
(8) Pertsin, A. J.; Grunze, M. *Langmuir* **1994**, *10*, 3668.
(9) Vargas, M. C.; Giannozzi, P.; Selloni, A.; Scoles, G. *J. Phys. Chem. B* **2001**, *105*, 9509.
(10) Yourdshahyan, Y.; Rappe, A. M. *J. Chem. Phys*. **2002**, *117*, 825.
(11) Vericat, C.; Vela, M. E.; Salvarezza, R. C. *Phys. Chem. Chem. Phys*. **2005**, *7*, 3258.
(12) Kautz, N. A.; Kandel, S. A. *J. Am. Chem. Soc*. **2008**, *130*, 6908.
(13) Maksymovych, P.; Sorescu, D. C.; Yates, J. T. *Phys. Rev. Lett*. **2006**, 97.
(14) Maksymovych, P.; Yates, J. T. *J. Am. Chem. Soc*. **2008**, *130*, 7518.
(15) Yu, M.; Bovet, N.; Satterley, C. J.; Bengio, S.; Lovelock, K. R. J.; Milligan, P. K.; Jones, R. G.; Woodruff, D. P.; Dhanak, V. *Phys. Rev. Lett*. **2006**, 97.
(16) Cossaro, A.; Mazzarello, R.; Rousseau, R.; Casalis, L.; Verdini, A.; Kohlmeyer, A.; Floreano, L.; Scandolo, S.; Morgante, A.; Klein, M. L.; Scoles, G. *Science* **2008**, *321*, 943.
(17) Gronbeck, H.; Hakkinen, H.; Whetten, R. L. *J. Phys. Chem. C* **2008**, *112*, 15940.
(18) Wang, J. G.; Selloni, A. *J. Phys. Chem. C* **2007**, *111*, 12149.
(19) Mazzarello, R.; Cossaro, A.; Verdini, A.; Rousseau, R.; Casalis, L.; Danisman, M. F.; Floreano, L.; Scandolo, S.; Morgante, A.; Scoles, G. *Phys. Rev. Lett*. **2007**, 98.
(20) Gronbeck, H.; Hakkinen, H. *J. Phys. Chem. B* **2007**, *111*, 3325.
(21) Molina, L. M.; Hammer, B. *Chem. Phys. Lett*. **2002**, *360*, 264.
(22) Torrelles, X.; Barrena, E.; Munuera, C.; Rius, J.; Ferrer, S.; Ocal, C. *Langmuir* **2004**, *20*, 9396.
(23) Voznyy, O.; Dubowski, J. J. *Langmuir* **2008**, *24*, 13299.
(24) Laibinis, P. E.; Whitesides, G. M.; Allara, D. L.; Tao, Y. T.; Parikh, A. N.; Nuzzo, R. G. *J. Am. Chem. Soc*. **1991**, *113*, 7152.
(25) Nuzzo, R. G.; Korenic, E. M.; Dubois, L. H. *J. Chem. Phys*. **1990**, *93*, 767.

absorption fine structure (NEXAFS)[26,27] and GIXRD measurements[28] indicate that thiols in the SAMs on Au (111) possess the densest possible packing, comparable to that of crystalline alkanes.[29,30] In our approach, thiol dense packing structures are obtained from molecular mechanics (MM) simulations in the absence of surface and then checked for commensurability with the known size of the surface unit cell. No attention to adsorption sites of the molecules is given at this step. Further fitting of crystalline structures of the surface and the monolayer is performed by introducing surface reconstructions (adatoms or vacancies), taking into account the known orbital shapes, bond lengths, and steric limits of sulfur and gold atoms, and, consequently, optimizing the geometry with DFT. The proposed method is simpler to implement and requires less computational effort than quantum mechanics/molecular mechanics (QM/MM) calculations,[5,16] since DFT and MM are never used simultaneously. Independently of the level of elaboration, current theoretical approaches inevitably conserve the amount of atoms in the unit cell, limiting in such a way possible outcomes of the simulation. Our approach offers a powerful complementary tool for a systematic search of initial guesses, helping to find reconstructions that optimize both thiol packing and thiol-surface interactions. Full details of the implementation of the method can be found in the Supporting Information and in our previous work.[23]

To generate possible dense packing structures of thiols, we used the DREIDING force field[31] as implemented in the Accelrys Discovery Studio package. The accuracy of MM calculations was tested on the most stable packing structure of polyethylene (orthorhombic unit cell). Obtained distances and angles between the alkane chains[23] are within 1% error from the most recent experiments.[32] The DFT geometry optimization and total energy calculations were performed for butanethiol and pentanethiol SAMs (hereafter, C4 and C5) using the SIESTA code[33] within the generalized gradient approximation (GGA) with Perdew−Burke−Ernzerhof (PBE) functional.[34] Optimized bases for Au,[35] C, H and S[36] were used. Surface slabs were modeled with four or five full Au layers and a vacuum region of ~30 Å. A (5 × 4) Monkhorst-Pack k-grid for the (3 × 2√3) unit cell was used. Forces on atoms were converged to 30 meV/Å. In order to reduce the basis set superposition error, "ghost" Au atoms (i.e., basis orbitals without actual atom) were placed in ideal bulk positions around adatoms for calculation of adatom formation energy and total energies of the "atop-adatom" models. Obtained lattice constant, bulk modulus, surface energy, and adatom formation energy were within the ranges of values reported previously.[10,18,21] Constant-current scanning tunneling microscopy (STM) images were simulated within the Tersoff−Hamann approach[37] for a range of biases from −3 to 3 eV. In-plane diffraction intensity maps were simulated using the ANA-ROD program,[38] taking into account the mirror and the 3-fold rotational symmetries of the substrate, following the procedure and notation conventions described in ref 22.

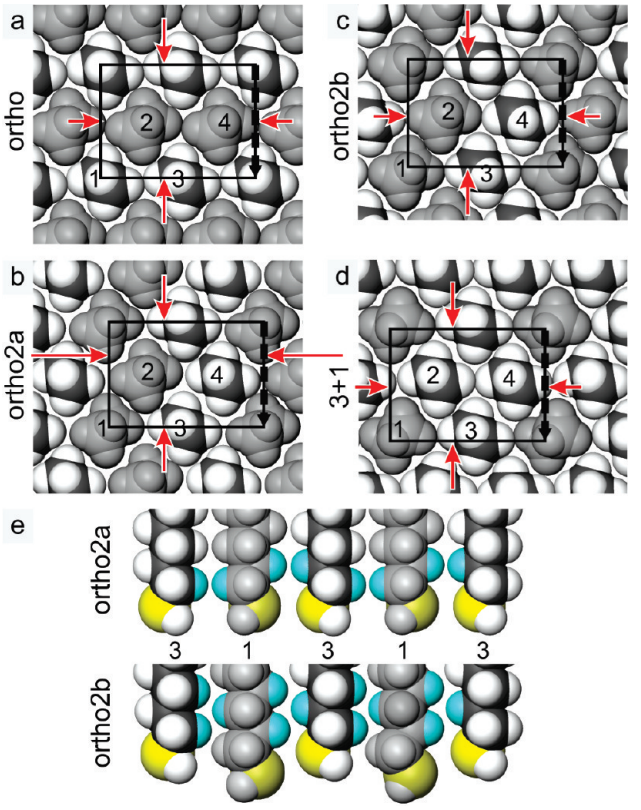

Figure 1. Prototypical alkanethiol packing structures commensurate with the (3 × 2√3) supercell of the Au (111) surface: panels a, b, c, and d show the view along thiol chains (i.e., ~35° off-normal to the surface, thiol tilt direction is indicated by bold dashed arrows) with thiols unit cell indicated. Red arrows indicate the compressive strain required to be imposed on relaxed packing structures to achieve full commensurability with the surface (the length of the arrows is proportional to the amount of strain, being 7% in the case of ortho2a structure). The difference between ortho2a and ortho2b packing structures and the incommensurability of the latter with an atomically flat surface is shown in panel e. Same numbering of chains as in panels b and c is used. Light blue hydrogen atoms are guides to the eye, darker and lighter shades of gray are used to distinguish the chains with different twists, and sulfur atoms are yellow.

3. Results

3.1. Prototypical Packing Structures. Figure 1 shows four of the six prototypical packing structures obtained by applying the proposed approach. The two structures not shown are the simple monoclinic, widely used in previous works to describe the √3 phase,[5−8] and a "3 + 1" structure similar to that shown in Figure 1d but with precession angle of 60° from the next nearest neighbor (NNN) thiol direction, and thus incompatible with GIXRD data.[28] For all of the structures the chain centers form ideal hexagons; however, sulfur positions deviate from this ideal pattern as a result of the a zigzag shape of thiol chains.

It should be noted, that all of the structures have some degree of misfit with the surface (red arrows with white outline in Figure 1). The tilt angle of ~35° needed to achieve full interlocking of chains[39] (also common to phases of Langmuir layers on liquids[29,30]) is larger than the 31.5° allowed by the area available

(26) Hahner, G.; Woll, C.; Buck, M.; Grunze, M. *Langmuir* **1993**, *9*, 1955.
(27) McGuiness, C. L.; Shaporenko, A.; Mars, C. K.; Uppili, S.; Zharnikov, M.; Allara, D. L. *J. Am. Chem. Soc.* **2006**, *128*, 5231.
(28) Fenter, P.; Eisenberger, P.; Liang, K. S. *Phys. Rev. Lett.* **1993**, *70*, 2447.
(29) Kaganer, V. M.; Mohwald, H.; Dutta, P. *Rev. Mod. Phys.* **1999**, *71*, 779.
(30) Kitaigorodskii, A. I. *Organic Chemistry Crystallography*; Consultants Bureau: New York, 1961.
(31) Mayo, S. L.; Olafson, B. D.; Goddard, W. A. *J. Phys. Chem.* **1990**, *94*, 8897.
(32) Takahashi, Y.; Kumano, T. *J. Polym. Sci. B* **2004**, *42*, 3836.
(33) Soler, J. M.; Artacho, E.; Gale, J. D.; Garcia, A.; Junquera, J.; Ordejon, P.; Sanchez-Portal, D. *J. Phys.: Condens. Matter* **2002**, *14*, 2745.
(34) Perdew, J. P.; Burke, K.; Ernzerhof, M. *Phys. Rev. Lett.* **1996**, *77*, 3865.
(35) Junquera, J.; Paz, O.; Sanchez-Portal, D.; Artacho, E. *Phys. Rev. B* **2001**, 64.
(36) Voznyy, O.; Dubowski, J. J. *J. Phys. Chem. B* **2006**, *110*, 23619.
(37) Tersoff, J.; Hamann, D. R. *Phys. Rev. Lett.* **1983**, *50*, 1998.
(38) Vlieg, E. *J. Appl. Crystallogr.* **2000**, *33*, 401.
(39) Ulman, A.; Eilers, J. E.; Tillman, N. *Langmuir* **1989**, *5*, 1147.

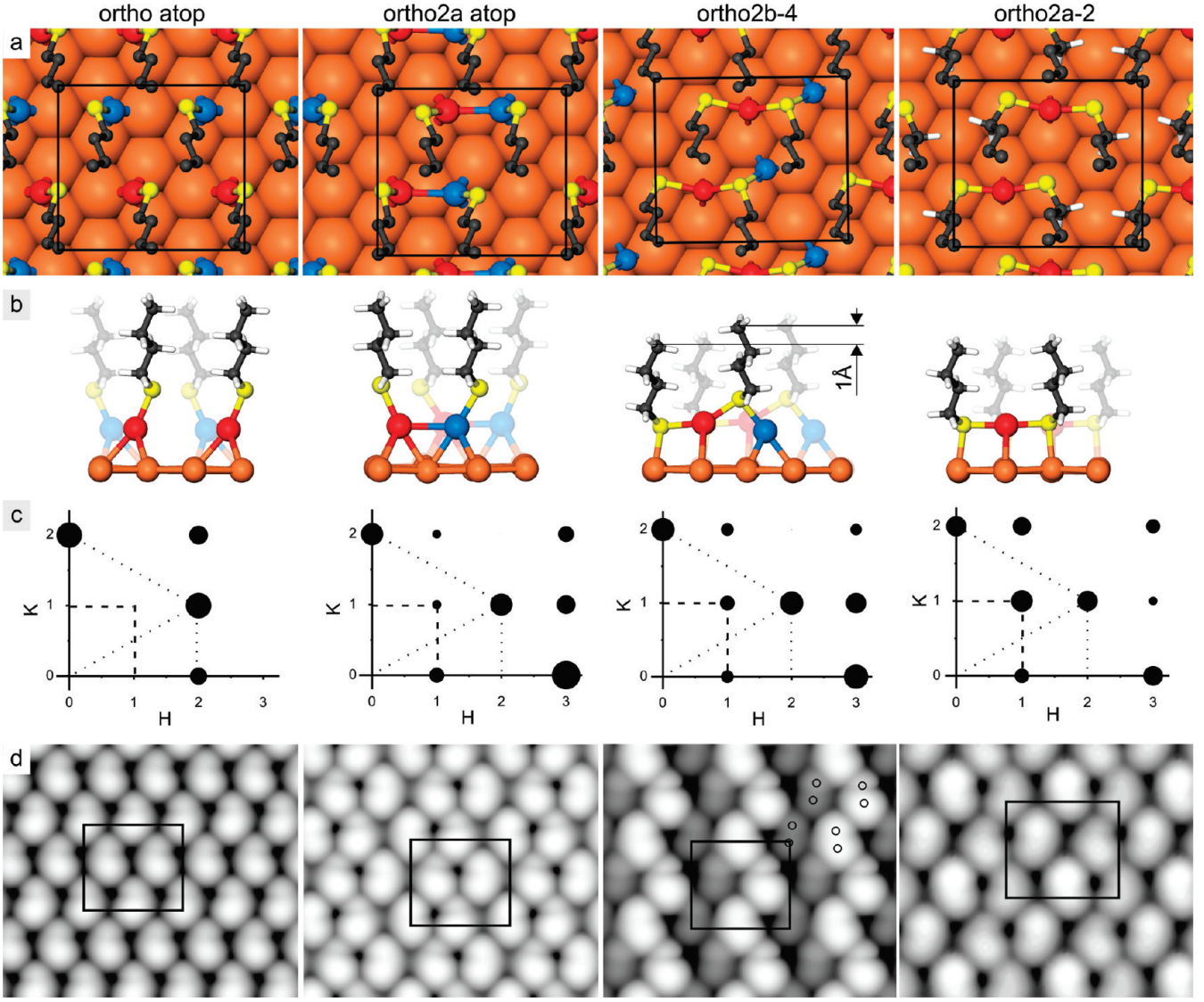

Figure 2. (a) Top and (b) side views of the DFT-relaxed structures. Red spheres: Au adatoms in fcc hollow or bridge adsorption sites: blue: Au adatoms in hcp hollow sites. Hydrogen atoms in panel a are omitted for clarity. For ortho2a-2, the bottommost H atoms are shown to reveal the absence of steric repulsion between them and adatoms. The $(3 \times 2\sqrt{3})$ cell is shown with solid line. (c) Simulated diffraction intensity maps for C10 thiols. Dotted lines indicate the $\sqrt{3}$ peaks, dashed line indicates the reciprocal $(3 \times 2\sqrt{3})$ unit cell. (d) Simulated STM images for C4 thiols produced for 0.8 eV bias (empty states) and 10^{-9} a.u.$^{-3}$ LDOS isosurface (located at 2.6 Å above the molecular apex). The shape of the bright protrusions in STM reproduces the positions of the two topmost hydrogen atoms (small circles) for chains with an even amount of carbon atoms, and reduces to a smaller circular shape for chains with odd amount of carbons, i.e., with only one topmost H.

per thiol on Au(111) surface.[4,30] Such a misfit of the SAM and surface unit cells along the tilt direction can be easily avoided by reducing the tilt angle at the expense of reduced chain interlocking.[39] The misfit in the perpendicular direction, however, can only be avoided by changing the twist of the chains, in agreement with the requirement of rotational distortions implied by IRS data.[25] Depending on the value of the misfit, this may result in significant disordering of the SAM.

The structure in Figure 1a (hereafter "ortho"), based on the orthorhombic packing observed experimentally for bulk alkanes,[29,30,32] cannot be fitted on an atomically flat surface. Dense packing restricts the positions of sulfur atoms so that not all of them can occupy the energetically favorable bridge face-centered cubic (fcc) site[5,9,10,18,21] (see Figure S2c for example). The DFT geometry optimization of such structure results in sulfur atoms falling down into bridge-fcc sites, destroying the dense packing. However, surface reconstructions with 1 or 2 adatoms per thiol are found to be compatible with dense packing. These structures are similar to inverted honeycomb (IHC) and honeycomb (HC) structures, proposed previously for monoclinic packing,[21] although, here the adatoms occupy both fcc and hexagonal close-packed (hcp) sites (see Figure 2a and Figure S3). The total energy differences for the structures discussed here are compiled in Table 1.

Positions of adatoms identical to those in "ortho-atop" structure (Figure 2a) were proposed for the "polymer" model[20] with sulfur atoms bridging the fcc (red) and hcp (blue) adatoms. This resulted in energetic gain compared to the flat-surface $\sqrt{3}$ structure due to reduced steric repulsion from the surface while still maintaining two bonds to the surface for sulfur. In the original "polymer" model, the two methylthiolates in the unit cell were tilted along the $\sqrt{3}$ direction (perpendicular to the one in our ortho-atop model) while in opposite directions to each other.[20] In our calculations we imposed the same tilt direction for all butanethiol chains, which resulted in a noticeable steric hindrance between thiols and made this structure isoenergetic to

Table 1. Relative Stability of the Structures with Respect to Adsorption on an Atomically Flat Surface[a]

		total energy difference, eV			
structure	Au atoms difference	this work	Molina, Hammer[b] ref [21].	Gronbeck, Hakkinen ref [20].	Gronbeck, Hakkinen, Whetten ref [17].
flat surface, mono ($\sqrt{3}$)	0	0	0	0	0
thiolate−vacancy, mono (HC)	−4	−0.55	−0.68		−0.53
thiolate−vacancy, ortho	−4	−0.35			
−Au−S− polymer	+4	1.30		−0.56[c]	−0.19[c]
atop adatom, mono (IHC)	+4	1.29	1.24	0.94	1.28
atop adatom, ortho	+4	1.30			
atop adatom, ortho2a	+4	1.22			
ortho2b-4	+4	0.4			
thiolate−adatom−thiolate, ortho2a-2	+2	−0.54		−0.46[c]	−0.84

[a] Energies per unit cell (four thiolates) are presented. Lower total energy corresponds to a more stable structure. Formation of adatoms (vacancies) is taken into account assuming exchange with the infinite bulk reservoir. Values from previous works are for methylthiolates, in current work they are for butylthiolates. [b] Results obtained using PW91 functional. [c] Exact geometries differ from the ones used in this work. See text for details.

the ortho-atop model (see Table 1). The optimized tilt angle for this model appeared to be only 10° (see the three-dimensional (3D) structure in the Supporting Information), while the tilt direction of the original polymer model is clearly incompatible with experimental data and our prototypical packing structures.

Packing structures shown in Figure 1b,c (hereafter "ortho2a" and "ortho2b", respectively) also exhibit orthorhombic symmetry. They differ from the ortho packing (Figure 1a) by the pattern of equivalent molecules within the unit cell, while the difference between the ortho2a and ortho2b themselves concerns the clockwise and counterclockwise twists with respect to the original monoclinic phase (see the Structures Generation Procedure in the Supporting Information). Different twist direction results in a better interlocking of the chains in ortho2b structure (see Figure 1e), and a smaller misfit with Au (111) surface along the NNN Au direction (Figure 1b,c). Similarly to ortho packing, molecules in ortho2a structure on an atomically flat surface cannot simultaneously accommodate bridge-fcc adsorption sites favored at low coverage. Nevertheless, ortho2a structure can easily adopt the atop-adatom geometry, requiring adatoms in a mixture of fcc and hcp sites (Figure 2a). In contrast to IHC structure, these adatoms are paired, insignificantly enhancing the stability of the structure (see Table 1).

The ortho2b (Figure 1c) and 3 + 1 (Figure 1d) structures are clearly not compatible with an atomically flat surface, since two and one chains in them, respectively, are shifted vertically, so that sulfur atoms are situated at different heights above the surface (Figure 1e). Such height modulation of S atoms was suggested by normal incidence X-ray standing wave (NIXSW) experiments.[40] The resulting end group height modulation might be also responsible for the observed STM contrasts.[41−44]

3.2. Atop-Adatom Model. On the basis of the obtained prototypical packing patterns, the exact structure of the recently proposed qualitative $c(4 \times 2)$ model involving thiolate−adatom species (four adatoms per unit cell)[15] can be resolved. Among our six prototypical packing structures, three can be adsorbed atop an adatom (namely, mono, ortho, and ortho2a) but only ortho and ortho2a require adatoms in a mixture of fcc and hcp sites (Figure 2a) as NIXSW data suggest.[15] Since the atomic scattering factor of Au is much higher than those of C and S, the resulting GIXRD maps would be dominated by adatoms (in our simulations for C10 thiols, addition of adatoms increases the peak intensities ~100 times). This, in turn, implies that it is enough to impose the centered rectangular symmetry[45] only on adatoms, while the chain twists can be arbitrary. Indeed, the absence of modulation in superlattice rods (and its presence in $\sqrt{3}$ rods) observed experimentally suggests that the superlattice peaks are not primarily the result of an ordering (twist) of the hydrocarbon chains, but rather that of S or Au atoms.[45] Among the three possible atop-adatom models, only ortho2a-atop structure has the required symmetry of adatoms (Figure 2a), resulting in a qualitatively correct diffraction map (i.e., has the missing (0;1), (2;0), (2;2) spots), as shown in Figure 2c (note that "mono-atop" not presented in the figure exhibits only $\sqrt{3}$ peaks). Nevertheless, all the three structures have practically identical energies (Table 1), providing no apparent reason for ortho2a-atop to be preferred. Since in the atop-adatom structures the adsorption geometries and chain twist angles of all the thiols are practically identical, no end group height modulation is observed in the simulated STM images (Figure 2d) in contrast to experimental observations.[41−44] Such a structure looks essentially like the $\sqrt{3}$ phase in STM, despite the underlying $c(4 \times 2)$ symmetry of the adsorption sites. Moreover, tilt of thiol chains causes a tilt of S−Au bonds as well (Figure 2b). Combined with a downward relaxation of adatoms, this reduces the distance from S to the nearest bulk Au plane to 1.9 Å (Figure S4), in contrast to 2.5 Å observed by NIXSW experiments.[15,46]

3.3. Alternative Model with Four Adatoms. Earlier work proposed a significantly different interpretation of NIXSW data,[40] requiring a ~0.8 Å height modulation of sulfur atoms, with the lower S atom situated atop Au, and the higher S close to the fcc site. The originally proposed "sulfur pairing model" compatible with this interpretation[40] was inconsistent with the more recent experimental data and thus was abandoned.[4,22] In contrast, our ortho2b and 3 + 1 structures have an intrinsic height modulation of ~1 Å of sulfur atoms. Figure 2a,b shows the structure based on ortho2b packing with four adatoms per unit cell (hereafter ortho2b-4) obtained by fitting it with the surface. It is similar to the previously reported $c(4 \times 2)$ structure on an atomically flat surface, derived using QM/MM calculations.[5] Addition of adatoms allowed for the improvement of packing density, while the formation of two bonds to Au for each S significantly enhanced the binding energy compared to the atop-adatom geometry. This resulted in ortho2b-4 structure being 0.82 eV per unit cell more stable (Table 1). In contrast to

(40) Fenter, P.; Schreiber, F.; Berman, L.; Scoles, G.; Eisenberger, P.; Bedzyk, M. J. *Surf. Sci.* **1998**, *413*, 213.
(41) Lussem, B.; Muller-Meskamp, L.; Karthauser, S.; Waser, R. *Langmuir* **2005**, *21*, 5256.
(42) Riposan, A.; Liu, G. Y. *J. Phys. Chem. B* **2006**, *110*, 23926.
(43) Zeng, C. G.; Li, B.; Wang, B.; Wang, H. Q.; Wang, K. D.; Yang, J. L.; Hou, J. G.; Zhu, Q. S. *J. Chem. Phys.* **2002**, *117*, 851.
(44) Zhang, J. D.; Chi, Q. J.; Ulstrup, J. *Langmuir* **2006**, *22*, 6203.
(45) Fenter, P.; Eberhardt, A.; Eisenberger, P. *Science* **1994**, *266*, 1216.
(46) Roper, M. G.; Skegg, M. P.; Fisher, C. J.; Lee, J. J.; Dhanak, V. R.; Woodruff, D. P.; Jones, R. G. *Chem. Phys. Lett.* **2004**, *389*, 87.

the QM/MM-derived flat-surface structure,[5] sulfur lateral and vertical positions in our model are compatible with NIXSW data.[40] Figure 2c,d shows the simulated GIXRD map (calculated for C10 thiols and averaged over three rotational domains to be directly comparable to experimental data[45]) and STM image for C4 thiols. Since adatoms possess the required centered rectangular symmetry, the diffraction intensity map is in qualitative agreement with experimental data (correct missing spots and relative intensities of the peaks).[45] The $\sqrt{3}$ peaks are stronger in the experimental map, as expected for $\sqrt{3}$ and $c(4 \times 2)$ phases coexisting on the surface.[22] Modulation of the headgroup and terminal group heights ~1 Å, combined with a zigzag pattern common to ortho2 structures, produces an STM image similar to those observed experimentally.[4,42,43]

3.4. Thiolate−Adatom−Thiolate Model. Adsorption of thiolate with S atom situated at the same level above the surface as a Au adatom, as observed for half of the chains in the ortho2b-4 geometry (see left chain in ortho2b-4 in Figure 2b), maximizes the binding energy of thiolate. Two bonds to the surface are formed, while adsorption atop Au allows avoiding steric repulsion, present in the bridge-fcc adsorption geometry on a flat surface.[21] Adsorption of all thiols in such atop geometry allows for the reduction in the amount of adatoms, resulting in the formation of thiolate−adatom−thiolate complexes, also observed experimentally in the low-density "striped" phase,[13] and compatible with NIXSW[15,40,46] and photoelectron diffraction (PED)[47] data. Previous works inspired by this geometry could not, however, find an appropriate structure of the SAM. Addition of the adatom resulted in the reduction of tilt from the correct 31° to ~20° and in the loss of dense packing due to disturbance of steric limits of the nearby CH_2 units.[18] Introduction of the ortho2a packing allows us to solve this problem. The resulting structure based on ortho2a packing and two adatoms per unit cell (hereafter ortho2a-2) is shown in Figure 2a,b. The opposite orientation of CH_2 units allows steric repulsion from adatoms to be avoided without affecting the dense packing. This structure is identical to the recently proposed $c(4 \times 2)$ model for methylthiolate,[17] however, deduced from completely different considerations.

The simulated diffraction intensity map of the proposed structure for C10 thiols is similar to that of the ortho2b-4 model (Figure 2c) and compares well with experimental data.[45] Despite equivalent adsorption sites, the simulated STM image in Figure 2d of the DFT-optimized structure exhibits a slight height modulation of thiol end groups. This modulation is due to the presence of a 7% misfit between the SAM and the surface, resulting in a slight deviation from ideal packing structure. The obtained zigzag pattern is similar to that typically observed experimentally; however, the ~0.1 Å height modulation in this model is significantly smaller than 0.4−0.7 Å observed experimentally.[41,42]

4. Discussion

All our models by construction possess a tilt angle compatible with IRS[24,25] and GIXRD[28] data. They also exhibit in one form or another the atop adsorption sites suggested by PED[47] and NIXSW.[15,46] We could not, however, find a suitable surface reconstruction involving thiolate−vacancy coexisting with thiolate−adatom complexes[16,18] compatible with any of the obtained prototypical packing structures. Discriminating between the proposed models based on available NIXSW or GIXRD data remains a complicated task because of controversies in the interpretation[15,40] or unavailability of the full experimental data sets to analyze the numerical values of the fit quality factors. Thus, we try to analyze the models from other points of view.

Our theoretical findings regarding the stability and structural properties of the atop-adatom model present arguments against its feasibility for explanation of the $c(4 \times 2)$ structure. Comparison of the stability of the models with different amount of adatoms, however, requires more attention. In previous works and in Table 1, stability of the new structures versus the flat-surface $\sqrt{3}$ phase was assessed assuming that adatoms come from an infinite bulk reservoir.[17,18,21] However, since there is no external source of gold atoms (as it could be in molecular beam epitaxy system), adatoms can only be pulled out from the surface itself,[16] lifting the herringbone reconstruction[13,48] or leaving a vacancy behind.[48,49] This leads to a 2-fold increase of the formation energy, from 0.57 eV for adatom coming from infinite bulk, to 1.1 eV for adatom−vacancy pair. Considering the increased adatom formation energies, all our structures, including the thiolate−adatom−thiolate model, become unstable compared to the flat-surface $\sqrt{3}$ model, in contrast to results from previous works.[17,20,21] Our calculated adatom formation energy reduces to ~0.8 eV at surface defects or step edges, a value comparable to that previously reported.[50] This value brings the thiolate−adatom−thiolate model ~0.1 eV lower in energy than flat-surface structure, while HC model remains clearly unfavorable (0.37 eV) since it requires the formation of 2 times the amount of defects.

The amount of adatoms present in the thiolate−adatom−thiolate structure corresponds to 0.17 monolayers of gold, compatible with recent experiments on SAM desorption using hydrogen flux.[12] The assumption that the creation of adatoms is accompanied by the creation of vacancies may also explain the presence of vacancy islands (etch pits) observed after SAM formation.[4,44,49] Taking into account that some initial amount of adatoms forms by lifting the herringbone reconstruction of the surface[13,48] and that, at step edges, formation of adatom does not leave a vacancy behind,[44] the amount of adatoms in the thiolate−adatom−thiolate model compares well to the 0.04 monolayers of etch pits reported previously and 0.07−0.1 monolayers estimated by us on the basis of the analysis of STM images from other works.[4,44,49]

Using similar reasoning, adatoms that are already present on the surface cannot escape into bulk[12] and can disappear only by attaching to a step edge. Thus, the $\sqrt{3}$ phase should contains the same amount of adatoms as $c(4 \times 2)$, since these phases were observed to interchange easily.[11] The atop-adatom IHC model[21] is a good candidate for a $\sqrt{3}$ counterpart of the $c(4 \times 2)$ phase presented by the ortho2b-4 model. However, the energy difference in this pair is too high (0.21 eV per thiol) to explain the coexistence of both phases on the surface.[11,51] On the other hand, it is impossible to form a $\sqrt{3}$ phase from thiolate−adatom−thiolate complexes. Recently it was proposed that disorder in their positions can explain the $\sqrt{3}$ GIXRD pattern,[19] although, no exact structure was proposed to test its appearance in STM.

In our simulations of STM images the thiolate−adatom−thiolate model looks very similar to the $\sqrt{3}$ phase. The exchange-correlation functional and the geometry relaxation procedure used in our DFT calculations for C4 thiols are not sensitive enough to the strain in the ortho2a-2 SAM to stipulate any

(47) Kondoh, H.; Iwasaki, M.; Shimada, T.; Amemiya, K.; Yokoyama, T.; Ohta, T.; Shimomura, M.; Kono, S. *Phys. Rev. Lett.* **2003**, 90.
(48) Dishner, M. H.; Hemminger, J. C.; Feher, F. J. *Langmuir* **1997**, *13*, 2318.
(49) Poirier, G. E.; Pylant, E. D. *Science* **1996**, *272*, 1145.
(50) Esplandiu, M. J.; Carot, M. L.; Cometto, F. P.; Macagno, V. A.; Patrito, E. M. *Surf. Sci.* **2006**, *600*, 155.
(51) Pflaum, J.; Bracco, G.; Schreiber, F.; Colorado, R.; Shmakova, O. E.; Lee, T. R.; Scoles, G.; Kahn, A. *Surf. Sci.* **2002**, *498*, 89.

noticeable deviation from the prototypical packing geometry. However, our MM simulations for longer chains have shown that a 7% shrinking of the prototypical ortho2a packing structure to the size of the unit cell imposed by Au (111) surface would result in rearrangement of chains, transforming the ortho2a structure into one of the less strained prototypical packings. Enforcement of the thiolate−adatom−thiolate binding geometry gives rise to disruption of ideal packing at the bottom of the chains and a gradual change of chain twists to accommodate the monoclinic, ortho2b, or 3 + 1 structure near the chain termini (Figure S5). These changes may be potentially responsible for the $\sqrt{3}$,[11,52] 2 + 2 (zigzag), and 3 + 1[41,42,51] phases, respectively, observed by STM. Gauche defects at the bottom of the chains could also help to achieve ortho2b packing in the unit cell with two adatoms, although they are unlikely for short chain thiols where reduction of packing density would be less expensive energetically.

Variation of bias from −3 to 3 eV and the choice of local density of states (LDOS) isosurfaces used in our STM simulations did not result in any qualitative change of the obtained STM patterns (see also Figure S6), in contrast to experimental observations.[41,42,51] Introduction of vacancies on the surface and even detachment of the SAM from the surface did not affect the STM images, suggesting that topographic effects are more important than changes in LDOS (at least in the Tersoff−Hamann approach), in agreement with previous findings.[43] We expect that phenomena other than LDOS should be invoked to explain the change of STM contrast upon changing the bias, e.g., structural changes in the monolayer induced by the tip, as described above for the ortho2a-2 structure or as proposed previously.[44]

Among our prototypical structures, only ortho2b (Figure 2d) is compatible with the zigzag pattern observed experimentally.[41−43] Similar patterns can be obtained for monoclinic, ortho, and ortho2a structures by cutting the chains at different heights, i.e., introducing sp- and sp^3-like bonding configurations of sulfur. However, our DFT calculations suggest that sp-like geometry is much less stable than the sp^3-like one. High-resolution STM or constant-height imaging can potentially resolve the sp- versus sp^3-like bonding[43,51] by distinguishing CH-up versus CH_2-up orientation of the chain termini (Figure 2b,d, and Figure S7), and discriminate between the proposed packing structures.

GIXRD remains the most useful tool to assess the amount of adatoms at the interface. It can potentially verify whether a zigzag pattern observed in STM is the result of disruption of the ideal packing within the thiolate−adatom−thiolate model or is a consequence of the structure with more adatoms per unit cell and native ortho2b packing. It should be noted, however, that strong deviations from bulk positions of gold atoms in the top surface layers, reported to be up to 0.5 Å,[16,22] can induce a signal stronger than that from thiol chains, thus providing extra freedom to fit experimental data even with incorrect chain geometries. Another variation of GIXRD analysis based on direct comparison of simulated and experimental electron densities and capable of suggesting the positions of adatoms[38] can be particularly useful to overcome this drawback.

5. Conclusions

We have adapted our previously proposed approach for searching the SAM structure on surfaces with unknown reconstruction to alkanethiol SAMs on Au (111). Using the known dimensions and symmetry of the $c(4 \times 2)$ unit cell, we obtained six prototypical structures compatible with the constraint of thiol dense packing. On the basis of these prototypical packings, the exact structure for the atop-adatom model was deduced, and two new structures with two and four adatoms per unit cell were proposed. No definitive conclusion regarding the preferred model can yet be made. Available theoretical and experimental data favor the thiolate−adatom−thiolate bonding geometry. However, in order to be compatible with STM data, some disruption of the ideal packing in this model is required. Additional experiments using our prototypical packings as a starting point can help to resolve the longstanding controversy about the structure of the $c(4 \times 2)$ phase. Application of our approach to other SAM−substrate systems is envisioned.

Acknowledgment. We thank Xavier Torrelles for preliminary fits of our structures to experimental GIXRD data, and Peter Maksymovych for fruitful discussions. The funding for this research has been provided by the Natural Sciences and Engineering Research Council of Canada (STPGP 350501-07) and Canada Research Chair in Quantum Semiconductors Program (J.J.D.). Computational resources were provided by the Réseau québécois de calcul de haute performance (RQCHP).

Supporting Information Available: Description of the procedure for systematic generation of dense packing structures and their verification for commensurability with the surface, 3D structures of the discussed SAM models, and simulated STM images for different tunneling conditions and packing configurations. This material is available free of charge via the Internet at http://pubs.acs.org.

(52) Torrelles, X.; Vericat, C.; Vela, M. E.; Fonticelli, M. H.; Millone, M. A. D.; Felici, R.; Lee, T. L.; Zegenhagen, J.; Munoz, G.; Martin-Gago, J. A.; Salvarezza, R. C. *J. Phys. Chem. B* **2006**, *110*, 5586.